PNAS RESEARCH ARTICLE | CELL BIOLOGY

lncRNA *BREA2* promotes metastasis by disrupting the WWP2-mediated ubiquitination of Notch1

Zhen Zhang[a,b,c,1], Yun-xin Lu[d,1], Fangzhou Liu[a,b,c,1], Lingjie Sang[a], Chengyu Shi[a], Shaofang Xie[e], Weixiang Bian[e], Jie-cheng Yang[a], Zuozhen Yang[a], Lei Qu[a], Shi-yi Chen[a], Jun Li[f], Lu Yang[g], Qingfeng Yan[a], Wenqi Wang[h], Peifen Fu[i], Jianzhong Shao[a], Xu Li[e,2], and Aifu Lin[a,b,c,j,k,2]

Edited by Christopher A. Maher, Genome Institute at Washington State University, St. Louis, MO; received April 20, 2022; accepted January 12, 2023 by Editorial Board Member Natalie G. Ahn

Notch has been implicated in human cancers and is a putative therapeutic target. However, the regulation of Notch activation in the nucleus remains largely uncharacterized. Therefore, characterizing the detailed mechanisms governing Notch degradation will identify attractive strategies for treating Notch-activated cancers. Here, we report that the long noncoding RNA (lncRNA) *BREA2* drives breast cancer metastasis by stabilizing the Notch1 intracellular domain (NICD1). Moreover, we reveal WW domain containing E3 ubiquitin protein ligase 2 (WWP2) as an E3 ligase for NICD1 at K1821 and a suppressor of breast cancer metastasis. Mechanistically, *BREA2* impairs WWP2–NICD1 complex formation and in turn stabilizes NICD1, leading to Notch signaling activation and lung metastasis. *BREA2* loss sensitizes breast cancer cells to inhibition of Notch signaling and suppresses the growth of breast cancer patient-derived xenograft tumors, highlighting its therapeutic potential in breast cancer. Taken together, these results reveal the lncRNA *BREA2* as a putative regulator of Notch signaling and an oncogenic player driving breast cancer metastasis.

therapeutic target | metastasis | lncRNAs | Notch signaling | ubiquitination

Metastasis, the spread of tumor cells from primary tumor sites followed by their colonization at a new site, is responsible for most cancer-related deaths and confers resistance to existing therapeutic agents in multiple cancers (1). To colonize distant organs, cancer cells undergo progressive genetic and phenotypic changes that drive dissemination from local tissues, subsequent entry into the bloodstream and survival in the circulation, and initiation of micrometastases (2, 3). This process relies on overcoming the cellular suppressive machinery modulated by ectopic activation of metastasis-associated pathways (3–5). Among these pathways, Notch signaling is a driver of epithelial–mesenchymal transition (EMT), a cellular program that promotes tumor cell intravasation (6–10). However, the molecular mechanisms underlying Notch pathway-mediated metastasis remain to be elucidated. Identifying components of the Notch activation complex would provide insight into the molecular mechanisms that govern Notch-mediated activation of cancer metastasis.

Mammalian Notch signaling is initiated by receptor–ligand interactions between neighboring cells. Notch receptor activation results in the translocation of its intracellular domain (NICD) into the nucleus to induce the expression of downstream target genes (11, 12). Termination of Notch signaling is mediated through proteasome-dependent degradation of the NICD (13–18). However, the regulation of NICD stability in the nucleus remains largely uncharacterized. The Notch pathway controls central cellular processes, including stemness, differentiation, proliferation, and metastasis (19). Deregulation of Notch signaling due to frequent mutations and aberrant activation of Notch signaling components has been implicated in tumor initiation, maintenance, and chemoresistance (20, 21). Mutational activation of Notch1 leading to aberrant Notch1 intracellular domain (NICD1) production and nuclear translocation is frequently found in human T cell acute lymphoblastic leukemia (T-ALL) (21). Recent studies have also highlighted the potential role of Notch signaling in human breast cancer development (22). For example, conditional overexpression of constitutively active NICD1, NICD3, or NICD4 in mouse mammary tissues leads to the development of metastatic breast tumors (23). However, mutations in Notch pathway components are rare in breast cancer (10), suggesting that alterations in its regulators could play a role in this process. Because of these features, the Notch pathway is a compelling target for new anticancer drugs. Although several agents, such as monoclonal antibodies against Notch ligands and receptors, and small-molecule γ-secretase inhibitors (GSIs) have been developed to block oncogenic Notch activation, GSIs have limited applications in human diseases due to their failure to distinguish between Notch receptors I and II and their severe intestinal toxicity (24–26). Therefore, identifying regulators of Notch degradation will reveal potential therapeutic targets to specifically antagonize distinct Notch receptors.

Previous studies, including ours, have indicated that long noncoding RNAs (lncRNAs), as emerging important modulators, are involved in cell signaling pathways via associations

Significance

The nuclear NICD1-specific regulatory mechanism governing Notch activation remains to be clarified, and the lack of this basic understanding hampers efforts to develop strategies to treat Notch-dependent cancer. Here, we report that the long noncoding RNA *BREA2* sustains lung metastasis by promoting Notch transcriptional activity. *BREA2* stabilizes Notch1 in the nucleus by attenuating ubiquitination mediated by an E3 ligase, WWP2, leading to Notch activation and lung metastasis. Targeting *BREA2* sensitizes breast cancer to Notch inhibitors. Moreover, the results reveal that WWP2 is a potential breast cancer suppressor. These findings provide evidence of the molecular mechanisms mediated by Notch signaling activation via the lung metastasis-associated lncRNA *BREA2* and open the door for the development of therapeutic approaches based on lncRNA targeting.

The authors declare no competing interest.

This article is a PNAS Direct Submission. C.A.M. is a guest editor invited by the Editorial Board.

[1]Z.Z., Y.-x.L., and F.L. contributed equally to this work.

[2]To whom correspondence may be addressed. Email: linaifu@zju.edu.cn or lixu@westlake.edu.cn.

This article contains supporting information online at https://www.pnas.org/lookup/suppl/doi:10.1073/pnas.2206694120/-/DCSupplemental.

Published February 16, 2023.

with protein partners (27–31). Here, we report that the lncRNA *BREA2* plays a pivotal role in breast cancer progression and metastasis by antagonizing the E3 ligase WWP2 to protect NICD1 from proteasome-dependent degradation. Deficiency of *BREA2* sensitized cells to GSI-induced inhibition of Notch1 activity and impaired the growth of breast cancer patient-derived xenograft (PDX) tumors, highlighting its antimetastatic role. Collectively, our findings not only reveal a lncRNA as a key regulator of Notch signaling in breast cancer metastasis but also provide an antimetastatic therapeutic strategy.

Results

***BREA2* Is Highly Expressed in Advanced Breast Cancer and Promotes Breast Cancer Cell Invasion.** Aberrant expression of lncRNAs is associated with malignant progression (27, 29, 32, 33). To identify breast cancer metastasis-associated lncRNAs, we found a group of lncRNAs from the NCBI Gene Expression Omnibus (GEO) (ID: GSE110590) (34) that were up-regulated in invasive human breast cancer metastatic tissues (n = 67) compared with paired primary breast tumor tissues (n = 16). A total of 83 significantly up-regulated lncRNAs and 105 down-regulated lncRNAs were identified. In addition, we compared alterations in lncRNA expression between two sets of stage III triple-negative breast cancer (TNBC) tissues and paired adjacent noncancerous tissues based on a GEO dataset (ID: GSE60689) (35) and identified 1,381 up-regulated lncRNAs (clinicopathological features and specific molecular characteristics are listed in *SI Appendix*, Table S1). Eventually, after overlapping the lncRNAs screened from the above databases, 12 lncRNAs attracted our attention (*SI Appendix*, Fig. S1*A*).

To further confirm the promising lncRNAs involved in breast cancer metastasis, we used lung metastases as a selection system (3, 36). MDA-MB-231-Luc/Green fluorescent protein (GFP) cells were introduced into the lungs by tail vein injection to establish tumors. After 4 wk, entrained cancer cells were extracted from the lungs (denoted as LuM-1 cells) by fluorescence-activated cell sorting for a second round of generation and yielded secondarily derived cells termed LuM-2 cells (Fig. 1*A*). Compared to MDA-MB-231 parental cells, LuM-2 cells exhibited a greater metastasis capacity, as determined by both invasion assays in vitro and metastasis experiments in vivo (*SI Appendix*, Fig. S1 *B* and *C*). Therefore, we screened metastasis-associated lncRNAs by Real Time Quantitative PCR (RT–qPCR) in LuM-2 subpopulations. Among these lncRNAs, *BREA2* exhibited higher expression in the LuM-2 subpopulations than in the parental MDA-MB-231 cells (fold change > 2.0) relative to the known lung metastasis-related genes *LY6E*, *ID1*, *MMP2*, and *CXCL-1* (Fig. 1*B*). Consistent with this finding, only *BREA2* and *WT1-AS* were identified among these 12 lncRNAs in the lung metastasis dataset of the published GSE110590 (34) cohort. As shown in Fig. 1*C* and *SI Appendix*, Fig. S1*D*, *BREA2* but not *WT1-AS* exhibited higher expression in lung metastases than in primary breast tumors.

Next, we further evaluated the associations between the levels of the five top lncRNAs (Fig. 1*B*) and patient survival in our cohort of individuals with breast cancer obtained from the Sun Yat-sen University Cancer Center (SYSUCC cohort 1). Univariate regression analysis showed that the level of *BREA2* had hazard ratios (HRs) and *P* values with survival time indicating a significant correlation with survival time (Fig. 1*D*). Using Kaplan–Meier survival curves, we further verified that high *BREA2* expression was closely associated with unfavorable overall survival in The Cancer Genome Atlas database (*SI Appendix*, Fig. S1*E*). Together, these results demonstrated that *BREA2* is a poor prognostic factor in breast cancer and is associated with lung metastases.

The *BREA2* transcript is located on chromosome 8q24.3 between the protein-coding genes *ZNF707* and *CCDC166*. The published chromatin immunoprecipitation–sequencing data revealed relatively low peaks of histone H3 lysine 4 trimethylation (H3K4me3), histone H3 lysine 4 monomethylation (H3K4me1), and H3 lysine 27 acetylation (H3K27Ac) in the *BREA2* genome (37, 38) (Fig. 1*E*). These results indicate that *ZNF707* and *BREA2* were distinct genes with separate promoters, and *BREA2* may not perform epigenetic function in transcriptional regulation (39). Comparison of the NCBI RefSeq database with the genomic sequence showed that the *BREA2* transcript is generated via the removal of 961 bases from the 5′ region of exon 1 (*SI Appendix*, Fig. S1*F*). By RT–qPCR and RACE using flanking primers, we demonstrated the existence of an alternative splicing product of the expected size (*SI Appendix*, Fig. S1 *F* and *G*) and validated the alternative splicing model by sequencing. As shown in *SI Appendix*, Fig. S1 *H* and *I*, there were approximately 350 copies of RNA *BREA2* per MDA-MB-231 cell, similar to the contents of known functional lncRNAs, such as *LINK-A* (approximately 150 copies per MDA-MB-231 cell) (27).

To confirm the function of *BREA2* under a tumor-specific context, we surveyed its genetic alterations in multiple cancers. *BREA2* is amplified in breast cancer in addition to ovarian, esophageal, and liver cancers (*SI Appendix*, Fig. S1*J*). Notably, *BREA2* expression was elevated in TNBC (*SI Appendix*, Fig. S1*K*). In addition, we performed RT–qPCR and RNA in situ hybridization (RNAScope) on breast cancer tissue microarrays (clinicopathological features are listed in *SI Appendix*, Table S1) to examine *BREA2* expression in breast cancer. Consistently, the expression of *BREA2* was higher in breast cancer tissues than in paired adjacent tissues (*SI Appendix*, Fig. S1*L* and Fig. 1*F*). These results were confirmed by RT–qPCR in comparison between stage III/IV and stage I/II breast cancer and between metastatic (TnN > 0/M ≥ 0) and nonmetastatic (TnN0M0) breast cancer in SYSUCC cohort 1 (Fig. 1 *G* and *H*). Moreover, a higher level of *BREA2* was correlated with unfavorable recurrence-free survival and unfavorable overall survival (*SI Appendix*, Fig. S1*M*) in breast cancer patients.

The lncRNAs perform vital physiological functions based on their subcellular localization (30, 31, 40). RNA fluorescence in situ hybridization (FISH), RT–qPCR, and northern blot analysis showed that *BREA2* was localized predominantly in the nucleus, especially in the nucleoplasm (Fig. 1*I* and *SI Appendix*, Fig. S1 *N–P*). Loss of *BREA2* impaired the cell proliferation, invasion, and migration of human breast cancer cells (*SI Appendix*, Fig. S2 *A–E*). In contrast, ectopic expression of *BREA2* promoted breast cancer cell migration and invasion (*SI Appendix*, Fig. S2 *F–H*).

EMT, a process by which tumor-associated epithelial cells gain mesenchymal features, has a critical role in migration and invasion (3). To characterize the function of *BREA2* in breast cancer migration and invasion, we assessed the expression of several canonical mesenchymal markers in *BREA2* knockdown cells. Interestingly, the expression of *Vimentin*, *Fibronectin*, *Twist1*, *N-cadherin*, *MMP9*, and *SNAI2* (which are positively correlated with EMT) was significantly reduced in *BREA2* knockdown cells. In contrast, the expression of the canonical epithelial markers *E-cadherin*, *zonula occludens-1*, and *Occludin* was up-regulated in *BREA2* knockdown cells (*SI Appendix*, Fig. S2*I*). These findings indicated that *BREA2* plays a key role in breast cancer migration and invasion.

***BREA2* Interacts with NICD1 and Positively Regulates Notch Signaling.** To investigate the regulatory mechanism by which *BREA2* promotes breast cancer migration and invasion, we performed an RNA pull-down assay followed by MS to search for *BREA2*-associated proteins that might be involved in the metastatic process. By comparison of the *BREA2* precipitate with the antisense and the bead control precipitates, Notch1 was identified as a potential binding protein of *BREA2* (Fig. 2*A* and *SI Appendix*, Table S2). Their interaction was validated by the RNA–protein binding assays in vivo and in vitro (Fig. 2*B* and *SI Appendix*, Fig. S3*A*) and RNA immunoprecipitation (RIP) assays (Fig. 2*C*). Next, Notch1 truncations were used to

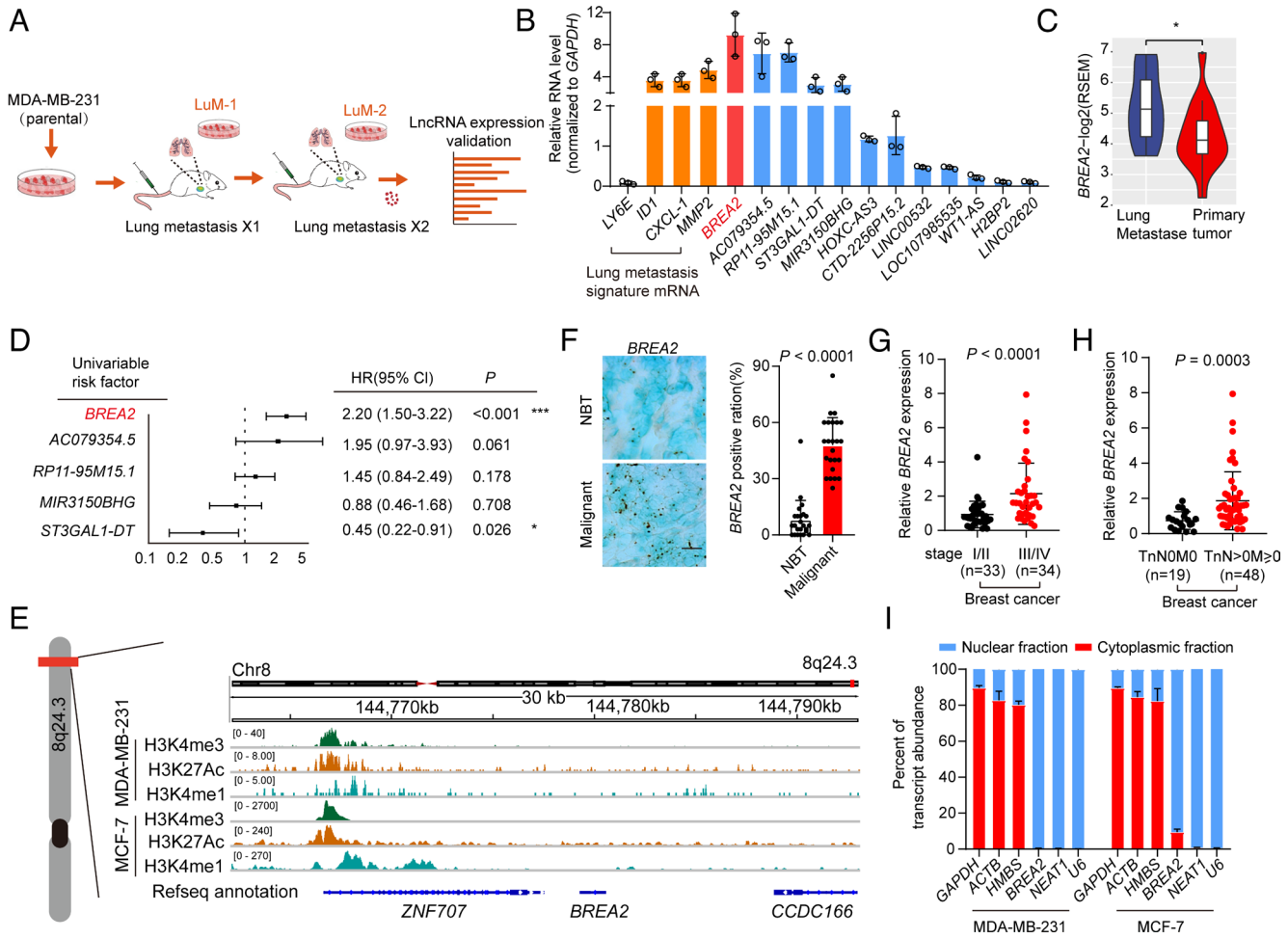

Fig. 1. Identification of the metastasis-associated lncRNA *BREA2* in breast cancer. (*A*) Experimental scheme for identifying lncRNAs involved in lung metastasis of breast cancer (detailed description in "*Materials and Methods*"). (*B*) RT–qPCR verification of the levels of lncRNA candidates in LuM-2 subpopulations compared with MDA-MB-231 parental cells (mean ± SD). Three independent experiments were performed. The positive controls of lung metastasis-associated genes (*ID1, CXCL-1*, and *MMP-2*) are shown as orange columns, and the negative control (*LY6E*) is shown as a white column (mean ± SD). *BREA2* is shown as a red column; the other confirmed candidates are shown as blue columns. (*C*) The expression level of *BREA2* in lung metastases and primary breast tumors was analyzed in the GSE110590 dataset (34) with the Wilcoxon rank-sum test, $*P < 0.05$. (*D*) Forest plot showing the HR (95% CI), and *P* values for the top five lncRNAs (fold change > 2.0) determined using univariate Cox proportional hazards regression analysis. HR, hazard ratio; CI. The bars correspond to the 95% CIs. n = 67, $*P < 0.05$, $***P < 0.001$. (*E*) Representation of the *BREA2* gene locus and its annotation in the current database. The snapshot of the region was derived from the University of California Santa Cruz (UCSC) Genome Browser (GRCH37/hg19, chr8:144,779,285-144,780,583). ChIP-seq data for H3K4me3, H3K4me1, and H3K27ac in the *BREA2* gene. (*F*) RNAScope® analysis of *BREA2* expression in adjacent normal breast tissues (NBTs) and malignant breast cancer tissues (n = 24 patients; Gehan–Breslow test). (Scale bar, 100 μm.) (*G* and *H*) RT–qPCR analysis of *BREA2* expression in breast cancer tissues (SYSUCC cohort 1; *SI Appendix*, Table S1; Mann–Whitney *U* test). (*I*) RT–qPCR analysis of *BREA2* expression in the cytoplasmic and nuclear fractions.

identify its binding regions with *BREA2*. Interestingly, *BREA2* directly interacted with the intracellular domain (NICD1) but not the extracellular domain (NECD1) of Notch1 (*SI Appendix*, Fig. S3*B*). In addition, the ankyrin (ANK) domain of NICD1 was required for its interaction with *BREA2* (Fig. 2 *D* and *E*). Moreover, the RNA *BREA2* secondary structure was determined by RNAstructure software (41), showing that *BREA2* contained three main branches. Several *BREA2* mutants were generated by deleting loop regions according to its secondary structure map, including loop1-deleted (D1; deletion of the sequence spanning nucleotides (nt) 1 to 225), loop2-deleted (D2; deletion of nt 229 to 364), and loop3-deleted (D3; deletion of nt 365 to 1,002) fragments (Fig. 2*F* and *SI Appendix*, Fig. S3*C*). The RNA pull-down assay based on these mutants indicated that *BREA2*-loop1 was required for the association of *BREA2* with NICD1 (Fig. 2*G* and *SI Appendix*, Fig. S3*D*).

Furthermore, the EMT process is a downstream event of Notch activation, and changes in EMT-associated gene expression could characterize the status of Notch signaling and the cell migration and invasion capacities. Depleting *BREA2* decreased the expression of several Notch target genes (e.g., HES1, HEY1, HEY2, and SNAI2) and increased the expression of E-cadherin, indicating that *BREA2* is a positive regulator of Notch signaling and EMT (Fig. 2*H* and *SI Appendix*, Fig. S3 *E* and *F*). In contrast, *BREA2* overexpression resulted in phenotypic changes opposite to those resulting from *BREA2* knockdown in breast cancer cells (*SI Appendix*, Fig. S3*G*). Moreover, *BREA2-FL* but not *BREA2-D1* rescued NICD1 and EMT marker expression in *BREA2* knockdown breast cancer cells (*SI Appendix*, Fig. S3 *H* and *I*), indicating that *BREA2* activated Notch activity and EMT via its loop1 structural region.

Aberrant expression of NICD1 and Jagged1 (Jagged Canonical Notch Ligand 1) is associated with poor outcomes of breast cancers characterized by EMT (42). Upon ligand binding, the Notch receptor is cleaved first by a disintegrin and metalloprotease (ADAM) family metalloproteases and then by the intramembrane γ-secretase complex to generate NICD, which in turn translocates into the nucleus to convert the DNA-binding protein RBP-J from a transcriptional repressor into an activator (43, 44). Depleting *BREA2* largely impaired Jagged1 (JAG1)-induced expression of Notch target genes *(HES1, HEY2, DTX1,* and *SNAI2)* and breast cancer cell invasion

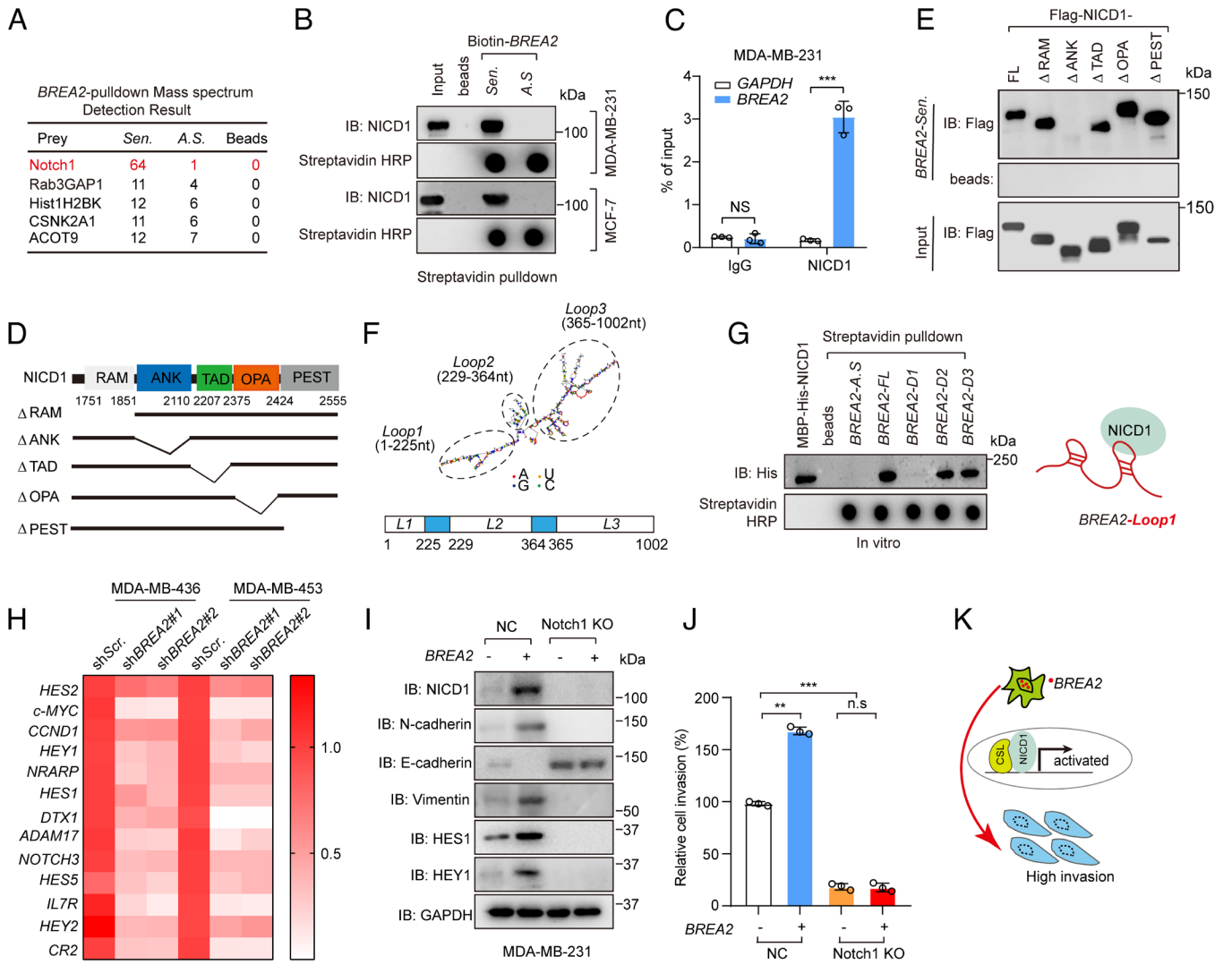

Fig. 2. Characterization of the lncRNA *BREA2* as a mediator of Notch1 transcriptional activity. (*A*) In vitro-transcribed biotinylated *BREA2* sense (*Sen.*) and antisense (*A.S.*) transcripts were incubated with MDA-MB-231 cell lysates for the RNA pull-down assay, which was followed by MS analysis to identify the *BREA2*-binding proteins. The representative candidates are listed. (*B*) In vitro-transcribed biotinylated *BREA2* sense and antisense transcripts were incubated with MDA-MB-231 and MCF-7 cell lysates for the RNA pull-down assay, which was followed by IB analysis. The input of biotin RNAs was detected by dot blotting using streptavidin–HRP. (*C*) An RIP assay was performed using the indicated antibody in MDA-MB-231 cells (mean ± SD). Three independent experiments were performed. ***$P < 0.001$, two-tailed Student's *t* test. (*D*) Schematic representation of NICD1 mutants. NICD1 mutants were generated as indicated amino acid positions according to the Notch region. RAM, RAM domain; ANK, ankyrin repeat domain; TAD, transcriptional activation region; OPA, OPA domain; PEST, PEST domain. (*E*) In vitro-transcribed biotinylated *BREA2* sense and antisense transcripts were incubated with HEK-293T cell lysates transfected with full-length (FL) Flag-NICD1 or the indicated Flag-NICD1 mutants for an RNA pull-down assay, followed by IB detection. (*F*) The secondary structure of *BREA2* was predicted by RNAstructure software. (*G*) In vitro-transcribed biotinylated *BREA2-FL* or *BREA2* mutants with partially deleted regions (D1, D2, and D3) were incubated with bacteria-purified recombinant MBP-His-NICD1 for an RNA pull-down assay, followed by IB detection. The input of biotin RNAs was detected by dot blotting using streptavidin–HRP. A schematic representation of the interaction between *BREA2* and NICD1 is shown (*Right*). (*H*) Heat map showing the normalized expression of Notch targets in *BREA2* knockdown MDA-MB-436 and MDA-MB-453 breast cancer cells. (*I*) IB analysis of the levels of the indicated proteins in Notch1-KO and control MDA-MB-231 cells transfected with *BREA2*. (*J*) Invasion assay in Notch1-KO or control MDA-MB-231 cells transfected with *BREA2* (mean ± SD). Three independent experiments were performed. **$P < 0.01$, ***$P < 0.001$, one-way ANOVA followed by Tukey's test. (*K*) Schematic representation of the function of *BREA2* in breast cancer invasion.

(*SI Appendix*, Fig. S3 *J–L*). Conversely, *BREA2* overexpression significantly increased the expression of the Notch target genes *HES1*, *HEY2*, *DTX1*, and *SNAI2* upon JAG1 treatment (*SI Appendix*, Fig. S3*M*). Notably, Notch1 elimination abolished the effect of *BREA2* on Notch activity and breast cancer cell invasion (Fig. 2 *I* and *J*). Collectively, these results suggested that *BREA2* mediated Notch activation to facilitate EMT in breast cancer (Fig. 2*K*).

***BREA2* Stabilizes NICD1 by Decreasing Its Ubiquitination.** Next, we aimed to elucidate the mechanism by which *BREA2* promotes Notch signaling in breast cancer cells. The expression of *BREA2* was positively correlated with that of NICD1 in a panel of breast cancer cells, indicating the functional relationship between *BREA2* and NICD1 (*SI Appendix*, Fig. S4*A*). Immunofluorescence and cell fractionation assays showed that depleting *BREA2* inhibited (Fig. 3 *A* and *B* and *SI Appendix*, Fig. S4*B*) but overexpressing *BREA2* increased NICD1 expression in the nucleus (*SI Appendix*, Fig. S4 *C–E*). Previous studies have revealed that NICD1 is cleared via continuous ubiquitination and proteasomal degradation (17, 45). Given that *BREA2* could not affect Notch1 mRNA levels (*SI Appendix*, Fig. S4*F*), we hypothesized that *BREA2* posttranslationally regulated NICD1 expression in breast cancer.

Indeed, treatment with the proteasomal inhibitor MG132 reversed the decrease in NICD1 expression in *BREA2* knockdown cells. We further verified that *BREA2* inhibited NICD1 proteasomal degradation in *BREA2*-overexpressing MDA-MB-231 cells (*SI Appendix*, Fig. S4*G*). Upon cycloheximide (CHX) treatment, the half-life of endogenous NICD1 was prolonged in the presence

of *BREA2* but was significantly diminished upon *BREA2* knockdown in several breast cancer cell lines, indicating that *BREA2* stabilized NICD1 in breast cancer cells (Fig. 3*C* and *SI Appendix*, Fig. S4 *H* and *I*). *BREA2* deficiency facilitated NICD1 ubiquitination (Fig. 3*D*), while *BREA2* overexpression reduced the ubiquitination of exogenous and endogenous NICD1 (*SI Appendix*, Fig. S4 *J* and *K*). Moreover, *BREA2* overexpression inhibited the Lys48-linked but not Lys63-linked polyubiquitination of NICD1 (Fig. 3*E*). Taken together, these findings demonstrated that *BREA2* binds NICD1 to reduce its Lys48-linked polyubiquitination and in turn stabilizes NICD1 in the nucleus (Fig. 3*F*).

WWP2 Functions as an E3 Ubiquitin Ligase for NICD1. To further identify the E3 ubiquitin ligase for NICD1, we immunoprecipitated Flag-tagged NICD1 in MCF-7 cells with or without *BREA2* overexpression prior to MS analysis to explore the potential binding proteins of NICD1. Among the identified binding partners of NICD1, several E3 ubiquitin ligases, including the known NICD1 E3 ligases Stub1 and Itch, were observed. Remarkably, WWP2 hits the highest score as a NICD1-interacting protein and gained our attention (Fig. 4*A* and *SI Appendix*, Table S3). Although other E3 ligases were also identified by our MS analysis, HUWE1 expression did not differ significantly between samples treated with or without *BREA2*, and both Stub1 and HECTD1 had relatively low abundances or nonsignificant differences in abundance. In addition, Itch has been reported to ubiquitinate the Notch receptor in lysosomes, and it has been reported that ectopic expression of WWP1 does not decrease TM/ICD1 expression (46, 47). Thus, we focused on WWP2 as the most likely candidate E3 ligase and determined its role in NICD1 ubiquitination mediated by *BREA2*. Next, the WWP2–NICD1 interaction was verified by in vivo and in vitro protein pull-down assays (*SI Appendix*, Fig. S5 *A–D*). Interestingly, the nuclear IP assay and proximity ligation assay (PLA) indicated that WWP2 and NICD1 were colocalized in the nucleus (Fig. 4 *B* and *C*).

As WWP2 is a HECT domain-containing E3 ligase, we examined the possibility that WWP2 ubiquitinated NICD1 in breast cancer cells (48). Indeed, WWP2 reduced nuclear NICD1 expression in a dose-dependent manner (Fig. 4*D* and *SI Appendix*, Fig. S5*E*). Supplementation with MG132 restored the basal NICD1 level in WWP2-overexpressing and WWP2-KO breast cancer cells, demonstrating that NICD1 was regulated by WWP2 via proteasomal degradation (Fig. 4*F* and *SI Appendix*, Fig. S5 *F* and *G*). Moreover, the half-life of endogenous NICD1 was diminished in WWP2-overexpressing breast cancer cells but increased in WWP2-KO cells upon CHX treatment (Fig. 4*E* and *SI Appendix*, Fig. S5*H*). Ectopic expression of WWP2 strongly down-regulated the expression of Notch downstream target genes, including *HES1*, *HES2*, *HEY2*, *CCND1*, and *SNAI2* (*SI Appendix*, Fig. S5*I*). Under protein-denaturing conditions, the abundances of ubiquitinated forms of exogenous NICD1 were increased by overexpression of wild-type WWP2 but not catalytically inactive $WWP2^{C838A}$ (Fig. 4*G*). These observations indicated that WWP2 functions as an E3 ligase for NICD1.

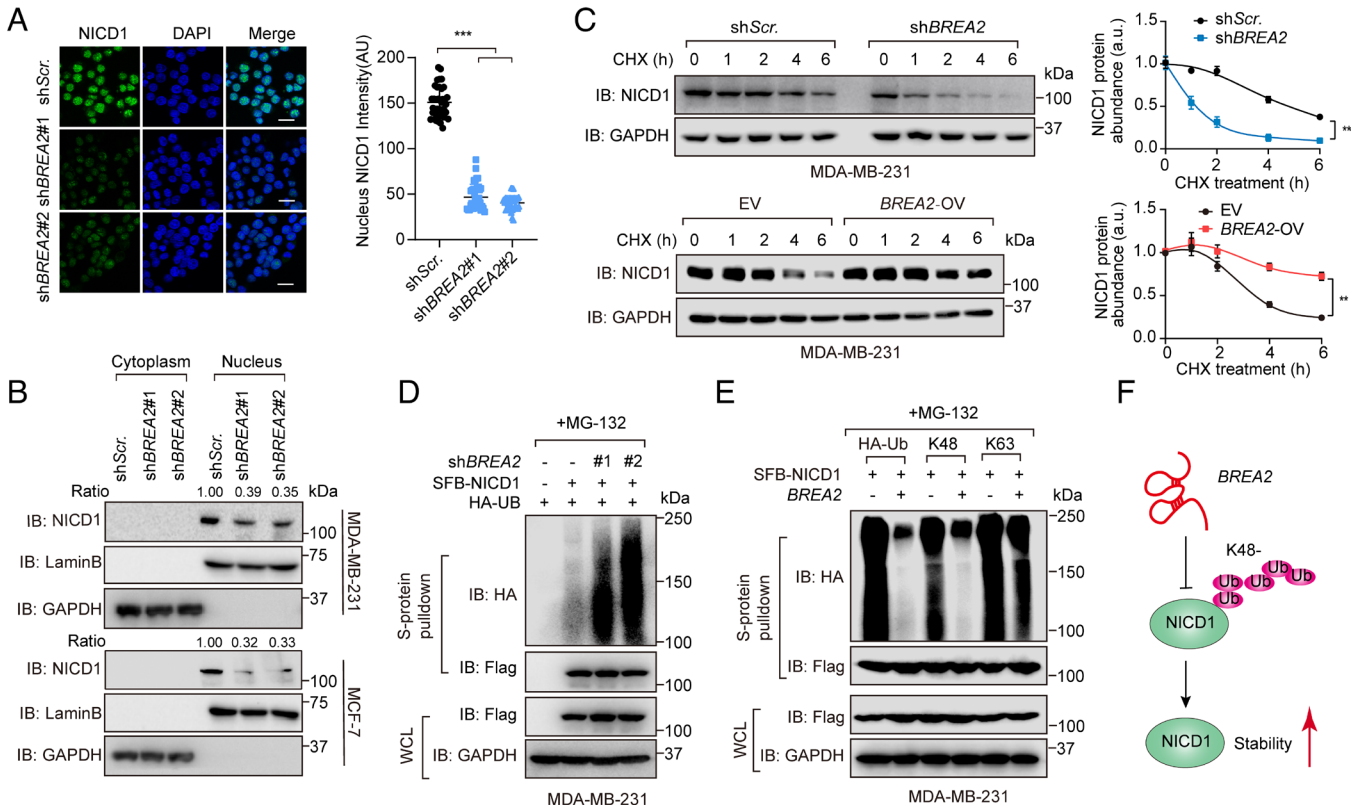

Fig. 3. *BREA2* affects the stability of NICD1 by preventing its ubiquitination. (*A*) Immunofluorescence analysis of NICD1 localization and expression in control and *BREA2* knockdown MDA-MB-231 cells. The fluorescence intensity was quantified to determine the mean intensity of NICD1 as indicated by the scattergram (mean ± SD). n = 38 cells, ***$P < 0.001$, one-way ANOVA followed by Tukey's test. (Scale bar, 20 μm.) (*B*) IB was used to evaluate NICD1 expression in cytoplasmic and nuclear extracts from control and *BREA2* knockdown cells. (*C*) The half-life of the NICD1 protein was measured in *BREA2* knockdown and *BREA2*-overexpressing MDA-MB-231 cells treated with CHX (20 μg/mL) at the indicated time points. Quantification of three independent experiments was shown (mean ± SD). **$P < 0.01$, two-way ANOVA test. (*D*) IB detection of SFB-NICD1 ubiquitination in *BREA2*-depleted and control MDA-MB-231 cells treated with MG132 (10 μM) for 6 h. HA-tagged ubiquitinated NICD1 was purified by immunoprecipitation using S-protein beads. SFB (S-tag–, Flag-tag–, and SBP-tag–fused) tagging was performed using the Gateway system (Invitrogen). Proteins with SFB tags could be recognized by anti-Flag antibody. (*E*) IB analysis of the ubiquitination status in *BREA2*-overexpressing MDA-MB-231 cells transfected with the K48-linked, K63-linked, or HA-Ub constructs and SFB-NICD1 as indicated. (*F*) Working model of *BREA2*-mediated NICD1 ubiquitination.

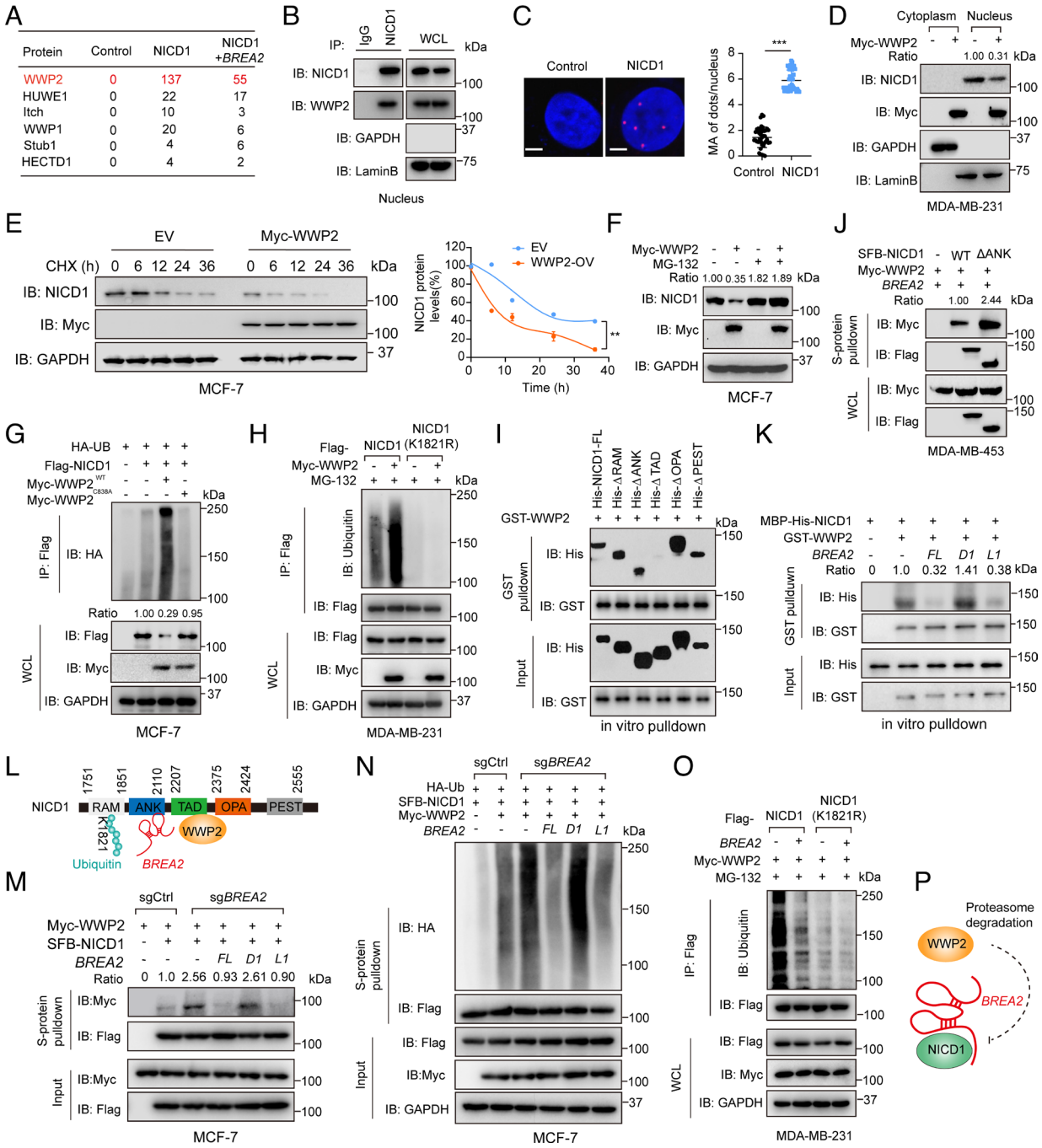

Fig. 4. *BREA2* disrupts the interaction between NICD1 and the E3 ligase WWP2. (*A*) MCF-7 cells stably transduced with Flag-tagged NICD1 or EV or with coexpression of Flag-NICD1 and *BREA2* were subjected to Flag immunoprecipitation and purification followed by mass spectrometry. The numbers of unique peptides of each protein in the immunoprecipitated products are shown. (*B*) Co-IP analysis of the interaction between NICD1 and WWP2 in MDA-MB-231 cells. IgG was used as a negative control. (*C*) PLA of the interaction between endogenous WWP2 and endogenous NICD1 in MDA-MB-231 cells. PLA signals are shown in red, and nuclei are shown in blue. (Scale bar, 5 μm.) Quantification of the mean area of WWP2/NICD1 PLA speckles is shown on a scattergram (mean ± SD). n = 40 cells, ***$P < 0.001$, two-tailed Student's *t* test. (*D*) IB analysis of NICD1 expression in cytoplasmic and nuclear extracts from MDA-MB-231 cells transfected with Myc-WWP2. (*E*) MCF-7 cells transfected with Myc-WWP2 were treated with CHX (20 μg mL^{-1}) and harvested at the indicated time points for IB analysis. Quantitative analysis of the NICD1 level relative to the GAPDH level is shown (mean ± SD). Three independent experiments were performed. **$P < 0.01$, two-way ANOVA. (*F*) MCF-7 cells transfected with Myc-WWP2 were treated with 10 μM MG-132 for 6 h, followed by IB analysis. (*G*) The level of ubiquitinated SFB-NICD1 was determined in MCF-7 cells transfected with wild-type or a catalytically inactive (C838A-mutant) Myc-WWP2. (*H*) Immunoprecipitation was performed to detect the ubiquitination of Flag-NICD1 and the K1821R mutant in MDA-MB-231 cells transfected with Myc-WWP2. Cells were treated with 10 μM MG-132 for 6 h before harvesting. (*I*) MCF-7 cells were transfected with the indicated His-tagged NICD1-mutant constructs. Whole-cell lysates were incubated with bacteria-purified recombinant GST-WWP2 followed by pulldown with GST resin and IB analysis. (*J*) Co-IP analysis of the interaction between Myc-WWP2 and the indicated SFB-NICD1 truncations in *BREA2*-overexpressing MDA-MB-453 cells treated with MG132 for 6 h before harvesting. (*K*) Recombinant GST-WWP2 and MBP-His-NICD1 proteins with additional equimolar amounts of FL, deletion 1 (D1), or *BREA2-loop1* (L1) were used for an in vitro GST pull-down assay. IB was performed to detect the interaction between WWP2 and NICD1. (*L*) Schematic diagram showing the direct interactions between NICD1 and *BREA2* and WWP2. (*M*) Co-IP analysis of the NICD1–WWP2 interaction in *BREA2*-null MCF-7 cells transfected with Myc-WWP2 or SFB-NICD1 and reexpressing *BREA2* loop mutants as indicated for 48 h. Cells were treated with 10 μM MG-132 for 6 h before harvesting. (*N*) The level of NICD1 ubiquitination was measured in *BREA2*-null MCF-7 cells transfected with SFB-NICD1, Myc-WWP2, and *BREA2* mutants as indicated for 48 h and treated with 10 μM MG-132 for 6 h before harvesting prior to IB analysis. (*O*) Immunoprecipitation was performed to detect the ubiquitination of Flag-NICD1 and the K1821R mutant in *BREA2*-overexpressing and control MDA-MB-231 cells transfected with Myc-WWP2 and Flag-NICD1 or Flag-NICD1-K1821R as indicated. Cells were treated with 10 μM MG-132 for 6 h before harvesting. (*P*) Graphical illustration of *BREA2*-WWP2–regulated NICD1 ubiquitination.

Based on the ubiquitination sites predicted by websites (http://smart.embl-heidelberg.de/) and identified by our MS analysis, a series of NICD1 K-R mutants were generated (*SI Appendix*, Table S4). NICD1^{K1821R} exhibited a longer half-life and decreased NICD1 ubiquitination level, suggesting that K1821 was an important ubiquitination site required for NICD1 stability (*SI Appendix*, Fig. S5*J* and Fig. 4*H*). Strikingly, NICD1^{K1821R} exhibited accelerated cell migration and cell colony formation compared to wild-type NICD1 (*SI Appendix*, Fig. S5 *K* and *L*). Ectopic expression of NICD1^{K1821R} greatly increased HES1-Luc reporter activity (*SI Appendix*, Fig. S5*M*). Collectively, these findings indicated that WWP2 enhances NICD1 ubiquitination at K1821. Next, an in vitro pull-down assay demonstrated that WWP2 likely binds to the TAD domain of NICD1 (Fig. 4*I*).

Given that *BREA2* stabilizes the NICD1 protein by interacting with its flanking ANK domain, we hypothesized that *BREA2* enhances the stability of NICD1 by impeding its WWP2-mediated ubiquitination and degradation. Indeed, *BREA2* overexpression disrupted the NICD1–WWP2 interaction in several breast cancer cell lines (*SI Appendix*, Fig. S6*A*), whereas *BREA2* could not bind WWP2 (*SI Appendix*, Fig. S6*B*). Moreover, NICD1$^{\Delta ANK}$, a mutant defective in the interaction with *BREA2*, bound more WWP2 in MDA-MB-453 cells (Fig. 4*J*). Supplementation with *BREA2-FL* but not with *BREA2-D1* inhibited NICD1–WWP2 complex formation, as shown by an in vitro pull-down assay (Fig. 4*K*). Additionally, reexpression of either *BREA2-FL* or *BREA2-loop1* inhibited the NICD1–WWP2 interaction in *BREA2*-null MCF-7 and MDA-MB-231 cells, whereas reexpression of *BREA2*-D1 did not (Fig. 4 *L* and *M* and *SI Appendix*, Fig. S6*C*). Immunofluorescence staining and PLA further confirmed that *BREA2* disrupted the WWP2–NICD1 association via its loop1 to stabilize NICD1 protein (*SI Appendix*, Fig. S6*D*). To investigate whether *BREA2* could stabilize NICD1 in breast cancer, we further examined the copy number of NICD1 in breast cancer cells. The results suggested that the *BREA2*:NICD1 ratio was 1:74 per MDA-MB-231 cell and 1:38 per MCF-7 cell (*SI Appendix*, Fig. S6*E*). These pieces of evidence indicated that *BREA2* might protect NICD1 from degradation by blocking WWP2–NICD1 complex formation.

To further determine whether the NICD1 ubiquitination status is affected by *BREA2*, we reexpressed *BREA2-D1*, *BREA2-FL*, and *BREA2-loop1* in *BREA2*-null MCF-7 cells. *BREA2*-loop1 was required for NICD1 stabilization (Fig. 4*N*). *BREA2* overexpression diminished WWP2-dependent ubiquitination of NICD1 (*SI Appendix*, Fig. S7 *A–C*) but not the NICD1^{K1821R} mutant (Fig. 4*O*) in several breast cancer cell lines. In contrast, *BREA2* knockout enhanced WWP2-dependent NICD1 ubiquitination (*SI Appendix*, Fig. S7*D*). Thus, *BREA2* stabilized NICD1 by preventing WWP2-mediated NICD1 ubiquitination at K1821.

We proposed that WWP2 might function as a tumor suppressor in breast cancer development. Next, we established MCF-7 cells stably expressing WWP2 or its C838A mutant. Ectopic expression of wild-type WWP2 but not WWP2^{C838A} reduced the expression of NICD1 and EMT markers in MCF-7 cells (*SI Appendix*, Fig. S7*E*) and inhibited breast cancer cell invasion (*SI Appendix*, Fig. S7 *F* and *G*). Conversely, depleting WWP2 increased the levels of NICD1 and EMT markers in MCF-7 and MDA-MB-231 cells (*SI Appendix*, Fig. S7 *H* and *I*) and promoted cell invasion and proliferation (*SI Appendix*, Fig. S7 *J–L*). However, ectopic expression of WWP2 reduced breast cancer cell growth (*SI Appendix*, Fig. S7*M*). To further assess the suppressive role of WWP2, we analyzed WWP2 expression in cancer samples. Oncomine database analysis showed that WWP2 expression was frequently decreased in multiple cancers, especially in breast cancer (*SI Appendix*, Fig. S7*N*), indicating that WWP2 functions as a suppressor in breast cancer. Collectively, these results demonstrated that *BREA2* stabilized NICD1 in the nucleus by preventing its WWP2-mediated degradation (Fig. 4*P*).

***BREA2* Promotes Breast Cancer Progression by Disrupting WWP2-Mediated NICD1 Degradation.** We next investigated whether the effects of *BREA2* on breast cancer cell invasion and growth were dependent on WWP2. Silencing *BREA2* enhanced the WWP2-mediated inhibitory effect on Notch signaling, as determined by assessing the activity of the Notch reporter genes TP1-luciferase and HES1-luciferase and the expression of the endogenous Notch target genes *HEY1* and *DTX1* (Fig. 5 *A* and *B* and *SI Appendix*, Fig. S8 *A–C*). Ectopic expression of *BREA2-FL* but not of *BREA2-D1* reversed WWP2-mediated downregulation of NICD1 protein expression and breast cancer cell invasion (*SI Appendix*, Fig. S8 *D–F*). However, *BREA2* depletion strongly enhanced WWP2-mediated inhibition of NICD1 expression and the expression of EMT marker in breast cancer cells (*SI Appendix*, Fig. S8*G*). Similar results were obtained in migration and Matrigel invasion assays after reexpressing *BREA2* mutants in *BREA2*-silenced MDA-MB-231 cells (Fig. 5*C* and *SI Appendix*, Fig. S8*H*), indicating that *BREA2* knockdown suppresses breast cancer cell migration and invasion.

To further clarify the role of *BREA2* in inducing a mesenchymal phenotype, we reexpressed *BREA2* mutants in *BREA2*-depleted MDA-MB-231 cells. Silencing *BREA2* enhanced the WWP2-mediated mesenchymal–epithelial transition phenotype, while the reintroduction of *BREA2-FL* resulted in a spindle-like, fibroblastic morphology, one of the main characteristics of cells undergoing EMT (Fig. 5*D*). Furthermore, the expression of both epithelial and mesenchymal molecular markers was evaluated by immunoblotting. The expression of E-cadherin, an epithelial marker, was significantly reduced by reexpression of *BREA2-FL* in *BREA2* knockdown MDA-MB-231 and MDA-MB-453 cells. In contrast, the expression of the mesenchymal markers Vimentin and N-cadherin was obviously up-regulated in cells with the reintroduction of *BREA2-FL* (Fig. 5*E* and *SI Appendix*, Fig. S8*I*). These results suggested that *BREA2* overexpression promotes EMT via WWP2 in breast cancer.

We next investigated whether the effects of WWP2 on breast tumor growth and metastasis are dependent on *BREA2*. To substantiate this hypothesis, MDA-MB-231 cells stably expressing WWP2 alone or with *BREA2* mutants were injected orthotopically into the mammary fat pads of immunodeficient mice. WWP2-expressing tumors grew slower and formed a reduced number of lung metastatic nodules, whereas *BREA2-FL* reversed the WWP2-induced inhibition of metastasis and growth (*SI Appendix*, Fig. S8 *J–L* and Fig. 5 *F–H*). Survival analysis showed that overexpression of *BREA2-FL* but not *BREA2-D1* in cells with stable ectopic expression of WWP2 shortened mouse survival compared with that of mice bearing WWP2-expressing tumors (Fig. 5*I*). Immunoblot (IB) analysis confirmed that NICD1 expression was increased in these metastatic tumors (*SI Appendix*, Fig. S8*M*). Moreover, *BREA2-FL* rescued WWP2-mediated inhibition of Notch activity in mice, with increased expression of Notch target genes such as *SNAI2*, *HES1*, *HEY1*, *DTX1*, and *CCND1,* as evidenced by RT–qPCR analysis (Fig. 5*J*). Collectively, these findings revealed the detailed mechanism of *BREA2*-mediated NICD1 turnover and cancer metastasis underlying the therapeutic potential of targeting *BREA2*.

***BREA2* Is a Potential Therapeutic Target for Breast Cancer Metastasis.** To determine the role of *BREA2* in treating Notch1-mediated metastasis, we investigated whether targeting *BREA2* would enhance the efficacy of the Notch inhibitor PF-03084014 in treating breast cancer metastasis (49). Interestingly, *BREA2* depletion enhanced the PF-03084014–induced inhibition of NICD1 expression, Notch downstream gene expression, and breast cancer cell migration (*SI Appendix*, Fig. S9 *A–C*). To further examine the role of *BREA2* in tumor metastasis in vivo, wild-type and *BREA2* knockdown MDA-MB-231-Luc cells were injected into nude mice via the tail vein (Fig. 6*A*). Bioluminescence imaging (BLI) showed that depleting *BREA2* greatly inhibited lung

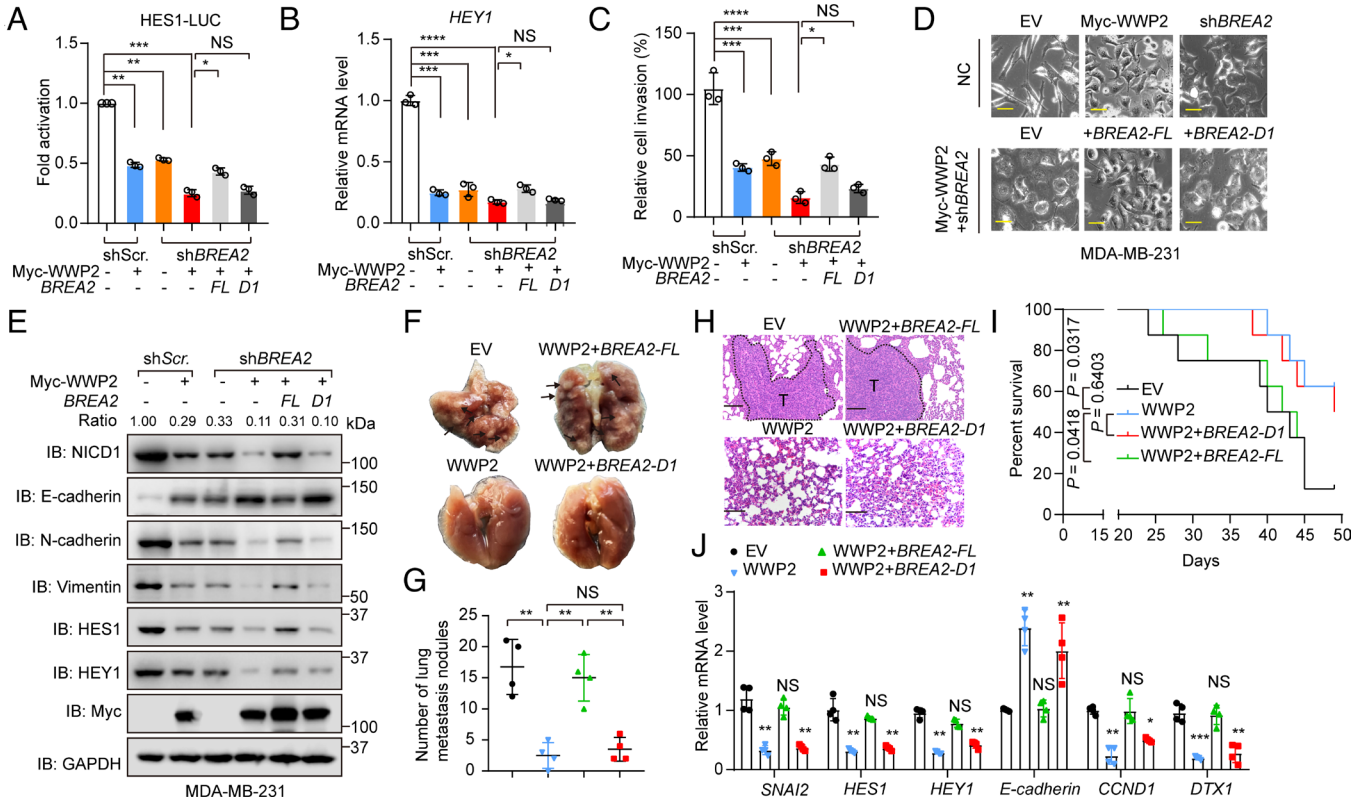

Fig. 5. *BREA2* inhibits the WWP2-mediated downregulation of Notch activity and promotes tumor growth and metastasis. (*A*) HES1-luciferase activity in *BREA2* knockdown and control MDA-MB-453 cells transfected with Myc-WWP2 and *BREA2* loop mutants as indicated (mean ± SD). Three independent experiments were performed. **P* < 0.05, ***P* < 0.01, ****P* < 0.001, one-way ANOVA followed by Tukey's test. (*B*) *HEY1* mRNA levels in *BREA2* knockdown and control MDA-MB-453 cells transfected with Myc-WWP2 and *BREA2* loop mutants as indicated (mean ± SD). Three independent experiments were performed. **P* < 0.05, ****P* < 0.001, *****P* < 0.0001, one-way ANOVA followed by Tukey's test. (*C*) Invasion assays in *BREA2* knockdown and control MDA-MB-231 cells transfected with Myc-WWP2 and *BREA2* loop mutants as indicated (mean ± SD). Three independent experiments were performed. **P* < 0.05, ****P* < 0.001, *****P* < 0.0001, one-way ANOVA followed by Tukey's test. (*D*) Images of the morphology of *BREA2*-silenced and control MDA-MB-231 cells transfected with Myc-WWP2 and *BREA2* loop mutants as indicated. (*E*) IB analysis of the expression of NICD1 and EMT markers and Notch target genes in *BREA2* knockdown and control MDA-MB-231 cells transfected with Myc-WWP2 and *BREA2* loop mutants as indicated. (*F*) Representative images of the mouse lungs showing metastatic nodules in the indicated groups. (*G*) Quantification of lung metastatic nodules in *F* (n = 4 mice/group). One-way ANOVA followed by Tukey's test, ***P* < 0.01. (*H*) Representative hematoxylin and eosin (H&E) images showing metastatic nodules in the lungs of mice in each group. (*I*) Tumor burden-based survival was plotted, with 500 mm^3 as the cutoff for moribundity. *P* values were determined by a two-sided log-rank test (n = 8 mice/group). (*J*) RT–qPCR analysis of Notch target genes, including *SNAI2, HES1, HEY1, E-cadherin, CCND1*, and *DTX1*, in each group (n = 4 mouse tumors). One-way ANOVA followed by Tukey's test, **P* < 0.05, ***P* < 0.01, ****P* < 0.001.

metastatic progression (Fig. 6*B*). Moreover, inhibition of *BREA2* reduced the number of lesions and average lesion surface area in lung sections in PF-03084014–treated mice (Fig. 6 *C* and *D*). RT–qPCR analysis further confirmed that *BREA2* deficiency enhanced the PF-03084014–induced downregulation of Notch downstream target genes in mice (Fig. 6*E* and *SI Appendix*, Fig. S9*D*). Histological analysis indicated that targeting *BREA2* decreased the area of metastatic lesions (Fig. 6*F*). Consistent with this finding, NICD1 expression was decreased in the *BREA2* knockdown groups treated with PF-03084014 compared to the other groups (Fig. 6 *F* and *G*). Furthermore, targeting *BREA2* using in vivo-optimized RNA interference (RNAi) significantly reduced tumor growth (*SI Appendix*, Fig. S9 *E–G* and Fig. 6 *H* and *I*), Notch1 activation, and angiogenesis (*SI Appendix*, Fig. S9*H* and Fig. 6*J*) in the PDX tumor model. These data demonstrated that *BREA2* deficiency sensitizes tumors to Notch inhibitors and suggested that *BREA2* is a potential therapeutic target in breast cancer.

High Expression of *BREA2* Correlates with Poor Clinical Outcomes in Breast Cancer Patients. We examined WWP2 expression in breast tumors and paired adjacent tissues by RT–qPCR and immunohistochemical (IHC) staining. Interestingly, WWP2 was down-regulated in advanced breast cancer tissues. Moreover, breast cancer tissues with higher WWP2 expression showed decreased Ki67 and NICD1 signals but increased E-cadherin signals (*SI Appendix*, Fig. S10 *A* and *B*). In addition, low WWP2 expression was correlated with unfavorable overall survival in breast cancer patients (*SI Appendix*, Fig. S10*C*), indicating that WWP2 suppressed breast cancer progression.

To examine whether *BREA2* is pathologically involved in breast cancer development, we categorized breast cancer tissues into the *BREA2*-high and *BREA2*-low groups by comparing their *BREA2* expression levels to the individual median. IHC staining showed that *BREA2* deficiency hindered tumorigenesis and metastasis, as indicated by Ki67, NICD1, N-cadherin, CD31, and E-cadherin staining (Fig. 7*A* and *SI Appendix*, Fig. S10*D*). Moreover, the expression level of *BREA2* was positively correlated with the levels of the Notch downstream genes *HEY2, HES1, SNAI2, NRARP, CCND1*, and *DTX1* (Fig. 7*B* and *SI Appendix*, Fig. S10*E*). Notably, IHC analysis of the NICD1 protein level and RNAScope analysis of the *BREA2* level revealed a statistically significant positive correlation (Fig. 7 *C–E*). Specifically, approximately 74% of the samples with activated Notch1 exhibited high *BREA2* expression, whereas 76% of the samples with inactivated Notch1 samples exhibited low *BREA2* expression (Fig. 7*E*). A further subgroup of individuals with breast cancer was classified to investigate the relationship between the *BREA2*–NICD1 axis and the survival rate. As shown in Fig. 7*F*, high levels of *BREA2* and NICD1 were strongly associated with a poor survival rate. Collectively, these data implied that the

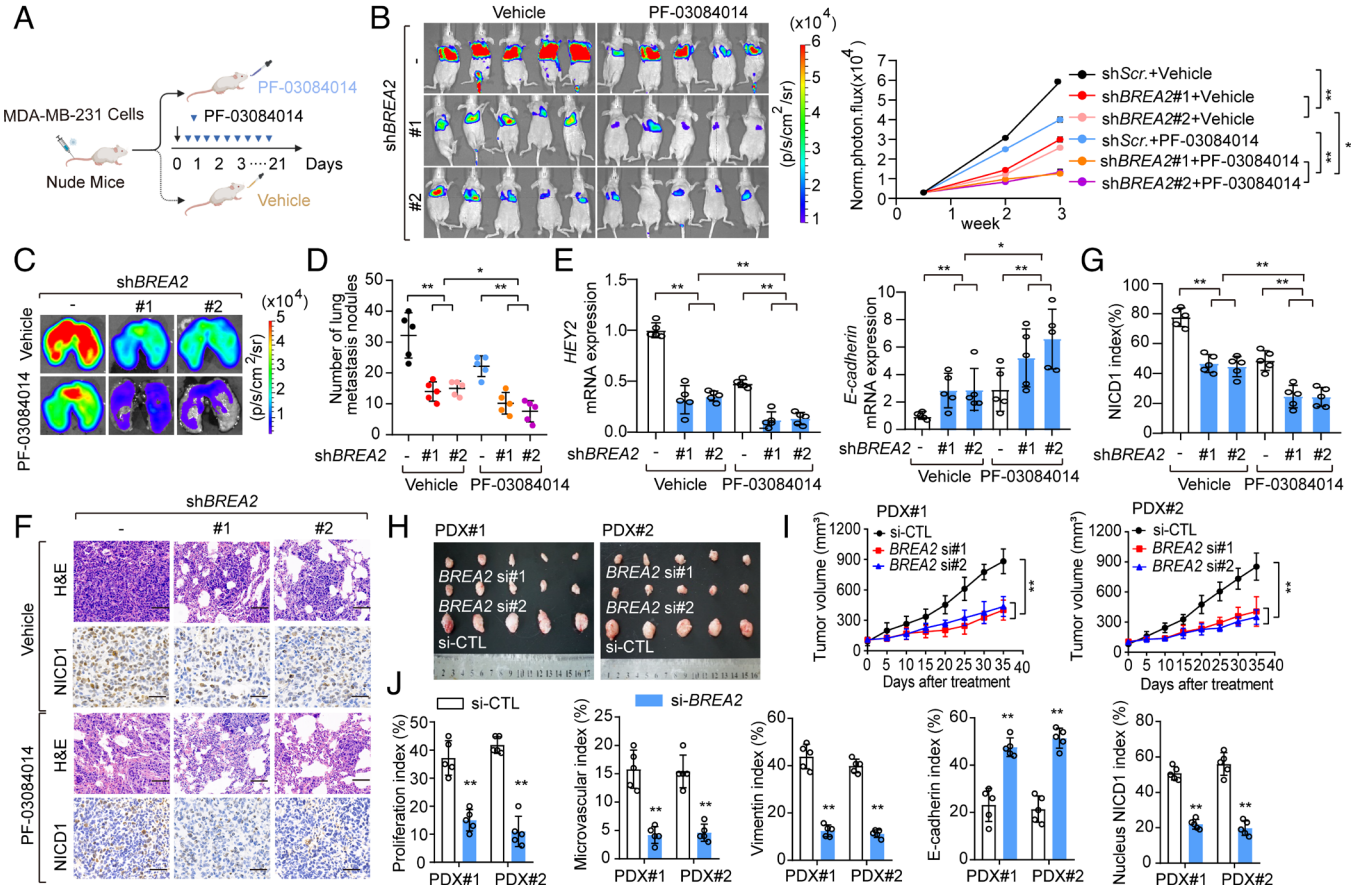

Fig. 6. *BREA2*-deficient breast cancer cells are sensitive to pharmacological inhibitors of Notch signaling. (*A*) Schematic diagram showing the strategy for administering the Notch inhibitor PF-03084014. Three days after tumor cell inoculation, the mice received an oral injection of either PF-03084014 (90 mg/kg) or vehicle twice daily for 3 wk. (*B*) Lung metastasis was evaluated by BLI. Normalized photon flux at the indicated time and representative images (*Left*) from five treated mice (mean ± SD). $*P < 0.05$, $**P < 0.01$, two-way ANOVA. (*C* and *D*) Representative bioluminescence lung images (*C*) and lung metastatic nodules (mean ± SD) in each group (n = 5 mice/group) (*D*) were shown. (Scale bar, 2 mm.) $*P < 0.05$, $**P < 0.01$, one-way ANOVA followed by Tukey's test. (*E*) RT–qPCR analysis of Notch target genes, including *HEY2* and *E-cadherin*, in the indicated experimental groups. n = 5 mouse tumors (mean ± SD). $*P < 0.05$, $**P < 0.01$, one-way ANOVA followed by Tukey's test. (*F*) Representative H&E and IHC staining images of the lung sections from every experimental group. (Scale bars, 1 mm and 100 μm for the lung (H&E) and NICD1 IHC images, respectively.) (*G*) The relative intensities of NICD1 IHC staining were quantified. n = 5 mouse tumors (mean ± SD). $**P < 0.01$, one-way ANOVA followed by Tukey's test. (*H* and *I*) In vivo analysis of tumors (*H*) and tumor growth (*I*) in each group (n = 5 mice/group) of mice subcutaneously implanted with tumor tissues from human breast cancer patients and injected with scrambled or *BREA2* RNAi constructs (20 mg/kg) every 3 d for 5 wk. $**P < 0.01$, two-way ANOVA. (*J*) The relative intensities of IHC staining were quantified by ImageJ software. n = 5 mouse tumors (mean ± SD). $**P < 0.01$, Mann–Whitney *U* test.

BREA2–Notch1 axis promotes breast cancer development, highlighting *BREA2* as a potential therapeutic target for breast cancer.

We further collected 23 patient-derived samples of lung and liver metastases and the matched primary breast tumors from the SYSUCC cohort (Cohort 2) and The First Affiliated Hospital of Zhejiang University (Cohort 3). RNAScope analysis indicated that the lung metastasis samples exhibited higher *BREA2* expression than the matched primary breast tumor samples, whereas the liver metastasis samples exhibited *BREA2* levels similar to those in the matched primary breast samples (Fig. 7 *G* and *H* and *SI Appendix*, Fig. S10 *F* and *G*). In addition, higher expression of *BREA2* in lung metastases was further confirmed in GEO datasets of human metastatic tumors (GSE14020 (50) and GSE54323 (51)) (*SI Appendix*, Fig. S10*H*). Collectively, these data suggested that the *BREA2*–NICD1 axis is involved in human breast cancer development, highlighting *BREA2* as a promising biomarker and therapeutic target for breast cancer (*SI Appendix*, Fig. S10*I*).

Discussion

The Notch signaling pathway controls cell growth, differentiation, and fate decisions, and its dysregulation has been linked to various human diseases, including T-ALL, chronic lymphocytic leukemia, colon cancer, and breast cancer (9, 52–54). Aberrant activation of Notch signaling in human cancers is associated with poor prognosis. To target Notch signaling, monoclonal antibodies and small-molecule GSIs have been developed (55). However, the limited efficacy and intestinal toxicity of these drugs limit their clinical application. Therefore, identifying new players involved in Notch signaling could reveal potential therapeutic targets. In this study, we focused on the regulation of Notch1 stability to discover targets for cancer treatment.

lncRNAs are involved in signal transduction and cancer development (28). Here, we identified several metastasis-associated lncRNAs by screening in a lung metastasis selection system. Notably, *BREA2* was identified as a regulator of cancer metastasis. Our results demonstrated that *BREA2* depletion significantly impaired the progression and metastasis of breast cancer, suggesting its importance in modulating metastatic development (Fig. 6). We also found that the expression of the lncRNA *BREA2* was increased in lung metastases in breast cancer patients (Fig. 7 *G* and *H*). Furthermore, a higher level of the lncRNA *BREA2* was common in Notch1-activated patients with breast cancer and was inversely correlated with prognosis (Fig. 7 *C*–*F*). All these data support our conclusion that the lncRNA *BREA2* has pleiotropic effects on breast cancer invasion and metastasis.

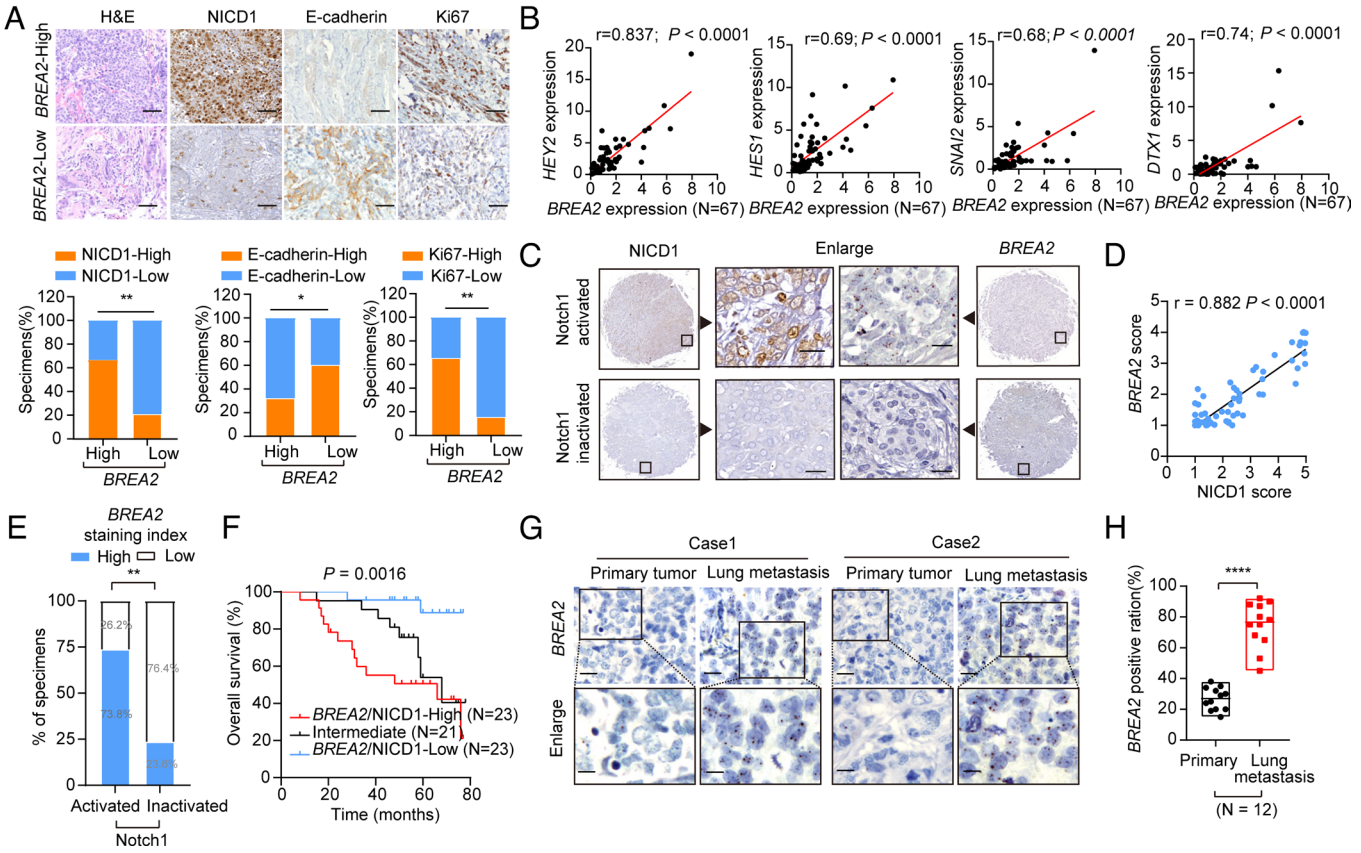

Fig. 7. Low *BREA2* expression benefits clinical outcomes in patients with breast cancer. (*A*) The expression of *BREA2*, NICD1, Ki67, and E-cadherin in primary human breast cancer specimens (SYSUCC cohort 1, n = 67) was evaluated by RT–qPCR and IHC analyses (*Upper*). (Scale bar, 100 μm.) The percentages of specimens showing low or high *BREA2* expression relative to NICD1, Ki67, and E-cadherin expression are shown (*Lower*). *$P < 0.05$, **$P < 0.01$, two-sided χ^2 test. (*B*) Correlations between the expression of *BREA2* and Notch target genes, including *HEY2, HES1, SNAI2,* and *DTX1,* in breast cancer tissues (SYSUCC cohort 1, n = 67). RNA levels were determined by RT–qPCR relative to U6 levels. Pearson correlation analysis. (*C*) IHC analysis of NICD1 and RNAScope analysis of *BREA2* in breast cancer tissue microarrays (SYSUCC cohort 1, n = 60); representative images of NICD1 and *BREA2* staining in the same patient samples are shown. (*D* and *E*) Correlations of *BREA2* levels with NICD1 protein levels. The 60 samples were classified into two groups (Notch1 activated and Notch1 inactivated) based on the level of NICD1 (n = 60). **$P < 0.01$, chi-square and Mann–Whitney *U* tests. (*F*) Individuals with breast cancer (n = 67) were divided into three groups according to the expression scores of NICD1 and *BREA2*. Overall survival curves were plotted by the Kaplan–Meier analysis with the log-rank test. (*G* and *H*) Representative images of *BREA2* staining were obtained by RNAScope® analysis in lung metastases and matched primary breast tumors (*G*) (n = 12 patients: Cohorts 2 and 3; *SI Appendix*, Table S1). (Scale bar, 10 μm.) The *BREA2* staining was quantified (*H*). ****$P < 0.0001$, Wilcoxon rank-sum test.

Therefore, the lncRNA *BREA2* was determined to have oncogenic activity.

Here, we report that the lncRNA *BREA2* positively up-regulates Notch1 transcriptional activity by preventing NICD1 polyubiquitination mediated by WWP2 and then inducing EMT (Figs. 4 and 5). Consistent with this finding, Notch1 signaling has been reported to constitute a key mechanism mediating breast cancer dissemination and metastasis in vivo (22, 56). Therefore, the identification of specific factors interacting with Notch signaling would facilitate a full understanding of the role of Notch in breast cancer.

Our results indicated that a higher level of the lncRNA *BREA2* was closely associated with higher Notch1 expression and was further inversely correlated with prognosis in patients with breast cancer (Fig. 7 *C*–*F*). Although Notch mutations occur frequently in several cancers, especially in T-ALL (21), we found that the lncRNA *BREA2* exhibited more than 19% amplification in metastatic breast cancer, and no mutations were observed in a Genome-Wide Association Studies (GWAS) of breast cancer (*SI Appendix*, Fig. S1*J*). A recent report indicated that Notch1 receptor mutations are clustered in the HD domain and PEST domain located in the C terminus of the Notch1 receptor in breast cancer (57). In this study, we found that the lncRNA *BREA2* binds to the ANK domain of Notch1 (Fig. 2*E*). Thus, Notch1 activation mediated by the lncRNA *BREA2* is dependent mainly on the abundance rather than the mutations of *BREA2* in breast cancer.

The lncRNAs constitute various types of transcripts, including long intergenic noncoding (linc) RNAs, natural antisense transcripts, and intronic lncRNAs. Furthermore, ncRNAs can be spliced from the mRNA precursors and originate from different genomic regions (58). In this study, we found that pre-*BREA2* harbors two exons derived from intron 2 of ENST00000527561.5 and is processed by splicing at the 3′ alternative splice site (ASS) to generate mature lncRNA *BREA2* (*SI Appendix*, Fig. S1*F*). A similar 3′ ASS model of lncRNAs and intronic lncRNAs, such as the lncRNA *PNUTS* and intronic lncRNA *Gm38257*, has been reported in several other studies (59, 60). Recent studies have also indicated that the biogenesis of lncRNAs is distinct from that of mRNAs and is related to their subcellular localization and functions (61). The precise mechanism underlying lncRNA biogenesis and processing remains to be further elucidated. Thus, the detailed biogenesis of the lncRNA *BREA2* requires further investigation.

lncRNAs have been reported to control gene expression at multiple levels, and the functions of lncRNAs are typically classified into four archetypal molecular mechanisms: signals, decoys, guides, and scaffolds (62). In this study, we found that the nuclear lncRNA *BREA2* stabilizes the NICD1 protein by impairing the NICD1–WWP2 association, thereby enhancing the NICD1 protein activity and its downstream target gene expression (Fig. 4). Our results indicated that the lncRNA *BREA2* acts as a "guard," a function distinct from the four existing archetypes. Archetypal signaling

lncRNAs, such as enhancer-like lncRNAs, participate in transcriptional activity via their epigenomic properties (39, 63). However, ChIP-seq analysis revealed that *BREA2* was not a putative enhancer, suggesting that the lncRNA *BREA2* does not perform its function via epigenetic regulation (Fig. 1*E*). Furthermore, the archetypal decoy lncRNAs, such as *GAS5* and *PANDA*, bind and titrate away protein targets, thus acting as "molecular sinks" to negatively regulate effectors (62). However, the lncRNA *BREA2* binds to NICD1 and stabilizes it, thereby enhancing effector activity. Our results indicated that the lncRNA *BREA2* performs the opposite function to decoy lncRNAs. Therefore, our results revealed a molecular archetype of lncRNA function in transcriptional regulation.

In this study, we found that the lncRNA *BREA2* attenuates the NICD1–WWP2 interaction, causing reduced ubiquitination and degradation of NICD1 (Fig. 4). WWP2 is an E3 ubiquitin ligase that belongs to the NEDD4-like protein family and is involved in regulating transcription, embryonic stem cell fate, cellular transport, and T cell activation processes (48). However, the regulation and function of WWP2 in human cancers remain to be elucidated. In prostate cancer, WWP2 facilitates PTEN degradation to promote cell proliferation (64). Notably, our work revealed WWP2 as an E3 ligase for NICD1 in breast cancer, indicating that, depending on the cellular context, WWP2 can be a tumor suppressor in breast cancer. We found that WWP2 down-regulated Notch signaling by promoting its ubiquitination and proteasome-dependent degradation in breast cancer.

Furthermore, WWP2 interacts with the NICD1 TAD domain, a region that is required for Notch transcriptional activity (65). Here, we demonstrated that the TAD domain of NICD1 likely binds to WWP2, indicating a function of the TAD domain in controlling Notch signaling (Fig. 4*I*). In the nucleus, *BREA2* likely binds to the neighboring region of the TAD, i.e., the ANK repeat domain, and disrupts the interaction between NICD1 and WWP2, which may be explained by steric hindrance due to the large and complex secondary structure of the lncRNA *BREA2*. WWP2, a member of the HECT domain family, has been reported to contain an N-terminal C2 domain followed by four WW domains and a C-terminal catalytic HECT domain. The N-terminal domains are responsible for substrate recognition. However, ubiquitin is transferred from the E2 enzyme to the C-terminal active site cysteine prior to transfer to the substrate, which may result in ubiquitination sites different from the binding sites (66). The precise mechanism of the HECT domain family remains to be further elucidated.

The identification of effective therapeutic strategies is critical to target drug-resistant cancers. Treatment with GSIs results in severe intestinal toxicity, limiting their clinical application, and the mechanism of GSIs toxicity remains to be explored. Our findings provide supporting evidence for the positive regulatory roles of *BREA2* in Notch activation, indicating that *BREA2* might be a promising therapeutic target for breast cancer. We previously demonstrated that depleting lncRNAs by in vivo-optimized RNAi exhibits a significant antitumor effect (28).

In this study, we designed an in vivo-optimized RNAi approach to target *BREA2* in a breast cancer PDX model. Silencing *BREA2* significantly reduced tumor growth, suggesting the translational potential of this strategy for cancers with Notch dysregulation (*SI Appendix*, Fig. S9*E*). Moreover, targeting lncRNAs by a locked nucleic acid (LNA)-based antisense oligonucleotide strategy has been a long-standing interest. Our previous work also indicated that lncRNA inhibition by LNAs exhibits significant efficacy and low toxicity against breast cancer progression (27, 33, 67), highlighting the utility of LNA-based therapies in targeting signaling-dependent tumorigenesis through lncRNAs. Thus, targeting lncRNAs by in vivo-optimized RNAi, LNA, or other approaches could constitute a promising strategy for clinical therapy. Collectively, our findings suggest *BREA2* as a potential therapeutic target for human cancers. It will be highly interesting to explore whether associations of lncRNAs with other oncogenic signaling-related biomolecules are involved in important physiological functions and can be targeted in the clinic.

Taken together, our research demonstrated that lncRNA *BREA2* acts as a key regulator of Notch1 signaling and revealed additional players in the Notch1 degradation. The findings of this study have significant implications regarding our understanding of breast cancer and lung metastasis pathogenesis. The effects of lncRNA *BREA2* on the invasion–metastasis cascade suggested that lncRNA *BREA2* could be an effective target for antimetastasis therapies.

Quantification and Statistical Analysis. The experiment was set up to use 3 to 5 samples/repeat per experiment/group/condition to detect a twofold difference with a power of 80% and a significance level of 0.05 by a two-sided test for significance. Representative images of IHC staining and immunoblotting are shown. Each of these experiments was independently repeated more than three times. Relative gene expression levels were normalized to *U6* or *GAPDH*. The results are reported as the mean ± SD of at least three independent experiments. Comparisons were performed using two-tailed paired Student's *t* test ($^{*}P < 0.05$, $^{**}P < 0.01$, and $^{***}P < 0.001$), as indicated in the individual figures. For survival analysis, the expression of the indicated genes was analyzed as a binary variable, and patients were divided into "high" and "low" expression groups. Kaplan–Meier survival curves were compared using the Gehan–Breslow test with Prism software (GraphPad, La Jolla, CA). The experiments were not randomized. All experiments were repeated three times independently, and the investigators were not blinded to the group allocations during the experiments and outcome assessment.

Study Approval. All patients provided informed written consent for specimen collection. Experiments were approved by the Ethics Committee of the SYSUCC and The First Affiliated Hospital of Zhejiang University School of Medicine. The animal experimental protocols in the study were approved by the Committee of Animal Ethics of the Zhejiang University.

Materials and Methods

Full methods and materials, including those used for protein recombination and purification, cloning, shRNA and RNAi, cell transfection, lentiviral gene transduction, cell lysis, immunoprecipitation, RIP, immunoblotting, RNA pulldown, mass spectrometry, RNAScope analysis, RNA FISH, northern blotting, immunofluorescence staining, Duolink® PLA fluorescence analysis, in vitro protein pulldown, colony formation assays, cell migration assays, dual-luciferase assays, immunohistochemistry, mice metastasis models, the lung metastasis selection system, and the in vivo human PDX model-based therapeutic study, as well as reagents and resources, are listed in *SI Appendix*.

Data, Materials, and Software Availability. All the MS and clinical data in this article has been included in the Supporting Information Datasets S1–S4. The survival analyses of *BREA2* levels were performed using TCGA database from online web server (https://www.xiantao.love/products/apply/c0b6febb-52dd-4525-970a-61bbe9e263ff/analyse/fc4754b7-d0fa-44af-9b0d-fa4e3fe1b7b3?title=5&code=2). Differentially expressed WWP2 in multiple cancers was acquired from the Oncomine database (https://www.oncomine.com/) with the threshold (P-value = 0.05, fold change =2, and gene ranking = 10%.). The genetic alterations of BREA2 in multiple cancers were obtained from the TCGA database using cBioPortal (https://www.cbioportal.org/). The reference sequence of *BREA2* was downloaded from the NCBI RefSeq database (https://www.ncbi.nlm.nih.gov/nuccore/NR_015445.1).

ACKNOWLEDGMENTS. We thank Prof. Y. Liu, Prof. J. Cai, Prof. L. Yu (Zhejiang University), Prof. C.C, and Prof. C.X (Chinese Academy of Sciences) for their support of and suggestions on this study. This study was funded by the National Science

Fund for Distinguished Young Scholars (32225014), "Lingyan" R&D Research and Development Project (2023C03023), National Key R&D Program of China (2021YFC2700903), National Natural Science Foundation of China (81672791 and 81872300), and Zhejiang Provincial Natural Science Fund for Distinguished Young Scholars of China (LR18C060002).

Author affiliations: [a]MOE Laboratory of Biosystem Homeostasis and Protection, College of Life Sciences, Zhejiang University, Hangzhou, Zhejiang 310058, China; [b]Cancer Center, Zhejiang University, Hangzhou, Zhejiang 310058, China; [c]Key Laboratory for Cell and Gene Engineering of Zhejiang Province, Zhejiang 310058, China; [d]Sun Yat-sen University Cancer Center, State Key Laboratory of Oncology in South China, Collaborative Innovation Center for Cancer Medicine, Guangzhou, Guangdong 510060, China; [e]Key Laboratory of Structural Biology of Zhejiang Province, Westlake Laboratory of Life Sciences and Biomedicine, Westlake University, Hangzhou, Zhejiang 310024, China; [f]Department of Pathology School of Medicine, The First Affiliated Hospital Zhejiang University, Hangzhou, Zhejiang 310003, China; [g]Department of Radiotherapy, Guangdong Provincial People's Hospital and Guangdong Academy of Medical Sciences, School of Medicine South China University of Technology, Guangzhou 510080, China; [h]Department of Developmental and Cell Biology, University of California, Irvine, CA 92697; [i]Department of Breast Surgery, The First Affiliated Hospital, School of Medicine, Zhejiang University, Hangzhou, Zhejiang 310003, China; [j]Breast Center of the First Affiliated Hospital, School of Medicine, Zhejiang University, Hangzhou, Zhejiang 310003, China; and [k]International School of Medicine, International Institutes of Medicine, The 4th Affiliated Hospital of Zhejiang University School of Medicine, Yiwu, Zhejiang 322000, China

Author contributions: X.L. and A.L. conceived and designed the research; Z.Z., Y.-x.L., F.L, L.S., C.S., J.-c.Y., Z.Y., L.Q., and S.-y.C. performed most of the biochemical and molecular experiments and bioinformatics analyses; Y.-x.L. performed breast cancer patient-derived xenograft tumor growth; J.L., L.Y., and P.F. collected breast cancer patient samples; Z.Y. and L.Q. conducted the bioinformatics analysis; Z.Z. and J.-c.Y. performed the xenograft experiments and immune-histochemical analyses; S.X. and W.B. conducted the MS analyses; Q.Y., W.W., J.S., and X.L. contributed to discussions and data interpretation; and Z.Z., F.L., X.L., and A.L. wrote the paper.

1. V. Padmanaban *et al.*, E-cadherin is required for metastasis in multiple models of breast cancer. *Nature* **573**, 439–444 (2019).
2. X. Tang *et al.*, SIRT7 antagonizes TGF-beta signaling and inhibits breast cancer metastasis. *Nat. Commun.* **8**, 318 (2017).
3. K. Gumireddy *et al.*, KLF17 is a negative regulator of epithelial-mesenchymal transition and metastasis in breast cancer. *Nat. Cell Biol.* **11**, 1297–1304 (2009).
4. P. S. Steeg, Metastasis suppressors alter the signal transduction of cancer cells. *Nat. Rev. Cancer* **3**, 55–63 (2003).
5. G. P. Gupta, J. Massague, Cancer metastasis: Building a framework. *Cell* **127**, 679–695 (2006).
6. A. M. Egloff, J. R. Grandis, Molecular pathways: Context-dependent approaches to Notch targeting as cancer therapy. *Clin. Cancer Res.* **18**, 5188–5195 (2012).
7. C. Lobry, P. Oh, M. R. Mansour, A. T. Look, I. Aifantis, Notch signaling: Switching an oncogene to a tumor suppressor. *Blood* **123**, 2451–2459 (2014).
8. K. Miao *et al.*, NOTCH1 activation compensates BRCA1 deficiency and promotes triple-negative breast cancer formation. *Nat. Commun.* **11**, 3256 (2020).
9. S. S. Sikandar *et al.*, NOTCH signaling is required for formation and self-renewal of tumor-initiating cells and for repression of secretory cell differentiation in colon cancer. *Cancer Res.* **70**, 1469–1478 (2010).
10. A. Stoeck *et al.*, Discovery of biomarkers predictive of GSI response in triple-negative breast cancer and adenoid cystic carcinoma. *Cancer Discov.* **4**, 1154–1167 (2014).
11. F. Ferrante *et al.*, HDAC3 functions as a positive regulator in Notch signal transduction. *Nucleic Acids Res.* **48**, 3496–3512 (2020).
12. A. Yatim *et al.*, NOTCH1 nuclear interactome reveals key regulators of its transcriptional activity and oncogenic function. *Mol. Cell* **48**, 445–458 (2012).
13. A. L. Guarnieri *et al.*, The miR-106b-25 cluster mediates breast tumor initiation through activation of NOTCH1 via direct repression of NEDD4L. *Oncogene* **37**, 3879–3893 (2018).
14. L. Li *et al.*, Ubiquitin ligase RNF8 suppresses Notch signaling to regulate mammary development and tumorigenesis. *J. Clin. Invest.* **128**, 4525–4542 (2018).
15. S. Pece *et al.*, Loss of negative regulation by Numb over Notch is relevant to human breast carcinogenesis. *J. Cell Biol.* **167**, 215–221 (2004).
16. S. Shin *et al.*, Deubiquitylation and stabilization of Notch1 intracellular domain by ubiquitin-specific protease 8 enhance tumorigenesis in breast cancer. *Cell Death Differ.* **27**, 1341–1354 (2020).
17. B. J. Thompson *et al.*, The SCFFBW7 ubiquitin ligase complex as a tumor suppressor in T cell leukemia. *J. Exp. Med.* **204**, 1825–1835 (2007).
18. W. Zhaojing *et al.*, Stabilization of Notch1 by the Hsp90 chaperone is crucial for T-cell leukemogenesis. *Clin. Cancer Res.* **23**, 3834–3846 (2017).
19. M. Roy, W. S. Pear, J. C. Aster, The multifaceted role of Notch in cancer. *Curr. Opin. Genet. Dev.* **17**, 52–59 (2007).
20. P. Ntziachristos, J. S. Lim, J. Sage, I. Aifantis, From fly wings to targeted cancer therapies: A centennial for notch signaling. *Cancer Cell* **25**, 318–334 (2014).
21. A. P. Weng *et al.*, Activating mutations of NOTCH1 in human T cell acute lymphoblastic leukemia. *Science* **306**, 269–271 (2004).
22. K. G. Leong *et al.*, Jagged1-mediated Notch activation induces epithelial-to-mesenchymal transition through Slug-induced repression of E-cadherin. *J. Exp. Med.* **204**, 2935–2948 (2007).
23. C. Hu *et al.*, Overexpression of activated murine Notch1 and Notch3 in transgenic mice blocks mammary gland development and induces mammary tumors. *Am. J. Pathol.* **168**, 973–990 (2006).
24. Y. Wu *et al.*, Therapeutic antibody targeting of individual Notch receptors. *Nature* **464**, 1052–1057 (2010).
25. Y. Ran *et al.*, Gamma-secretase inhibitors in cancer clinical trials are pharmacologically and functionally distinct. *EMBO Mol. Med.* **9**, 950–966 (2017).
26. D. C. Smith *et al.*, A phase 1 dose escalation and expansion study of Tarextumab (OMP-59R5) in patients with solid tumors. *Invest. New Drugs* **37**, 722–730 (2019).
27. A. Lin *et al.*, The LINK-A lncRNA activates normoxic HIF1alpha signalling in triple-negative breast cancer. *Nat. Cell Biol.* **18**, 213–224 (2016).
28. L. J. Sang *et al.*, LncRNA CamK-A regulates Ca(2+)-signaling-mediated tumor microenvironment remodeling. *Mol. Cell* **72**, 71–83.e7 (2018).
29. X. Zheng *et al.*, LncRNA wires up Hippo and Hedgehog signaling to reprogramme glucose metabolism. *EMBO J.* **36**, 3325–3335 (2017).
30. R. H. Li *et al.*, A phosphatidic acid-binding lncRNA SNHG9 facilitates LATS1 liquid-liquid phase separation to promote oncogenic YAP signaling. *Cell Res.* **31**, 1088–1105 (2021), 10.1038/s41422-021-00530-9.
31. L. Sang *et al.*, Mitochondrial long non-coding RNA GAS5 tunes TCA metabolism in response to nutrient stress. *Nat. Metab.* **3**, 90–106 (2021).
32. A. Lin *et al.*, The LINK-A lncRNA interacts with PtdIns(3,4,5)P3 to hyperactivate AKT and confer resistance to AKT inhibitors. *Nat. Cell Biol.* **19**, 238–251 (2017).
33. Z. Xing *et al.*, lncRNA directs cooperative epigenetic regulation downstream of chemokine signals. *Cell* **159**, 1110–1125 (2014).
34. M. B. Siegel *et al.*, Integrated RNA and DNA sequencing reveals early drivers of metastatic breast cancer. NCBI Gene Expression Omnibus. https://www.ncbi.nlm.nih.gov/geo/query/acc.cgi?acc=GSE110590. Deposited 14 February 2018.
35. Z. Xing *et al.*, lncRNA directs cooperative epigenetic regulation downstream of chemokine signals. NCBI Gene Expression Omnibus. https://www.ncbi.nlm.nih.gov/geo/query/acc.cgi?acc=GSE60689. Deposited 22 August 2014.
36. A. J. Minn *et al.*, Genes that mediate breast cancer metastasis to lung. *Nature* **436**, 518–524 (2005).
37. W. Xu *et al.*, Dynamic control of chromatin-associated m(6)A methylation regulates nascent RNA synthesis. *Mol. Cell* **82**, 1156–1168.e7 (2022).
38. K. Li *et al.*, Comprehensive epigenetic analyses reveal master regulators driving lung metastasis of breast cancer. *J. Cell Mol. Med.* **23**, 5415–5431 (2019).
39. W. Li, D. Notani, M. G. Rosenfeld, Enhancers as non-coding RNA transcription units: Recent insights and future perspectives. *Nat. Rev. Genet.* **17**, 207–223 (2016).
40. F. Liu *et al.*, Long non-coding RNA SNHG6 couples cholesterol sensing with mTORC1 activation in hepatocellular carcinoma. *Nat. Metab.* **4**, 1022–1040 (2022).
41. J. S. Reuter, D. H. Mathews, RNAstructure: Software for RNA secondary structure prediction and analysis. *BMC Bioinformatics* **11**, 129 (2010).
42. S. Shao *et al.*, Notch1 signaling regulates the epithelial-mesenchymal transition and invasion of breast cancer in a Slug-dependent manner. *Mol. Cancer* **14**, 28 (2015).
43. R. E. Moellering *et al.*, Direct inhibition of the NOTCH transcription factor complex. *Nature* **462**, 182–188 (2009).
44. G. van Tetering *et al.*, Metalloprotease ADAM10 is required for Notch1 site 2 cleavage. *J. Biol. Chem.* **284**, 31018–31027 (2009).
45. V. Close *et al.*, FBXW7 mutations reduce binding of NOTCH1, leading to cleaved NOTCH1 accumulation and target gene activation in CLL. *Blood* **133**, 830–839 (2019).
46. J. Chen *et al.*, Ogt controls neural stem/progenitor cell pool and adult neurogenesis through modulating Notch signaling. *Cell Rep.* **34**, 108905 (2021).
47. L. Puca, P. Chastagner, V. Meas-Yedid, A. Israel, C. Brou, Alpha-arrestin 1 (ARRDC1) and beta-arrestins cooperate to mediate Notch degradation in mammals. *J. Cell Sci.* **126**, 4457–4468 (2013).
48. H. M. Xu *et al.*, Wwp2, an E3 ubiquitin ligase that targets transcription factor Oct-4 for ubiquitination. *J. Biol. Chem.* **279**, 23495–23503 (2004).
49. C. C. Zhang *et al.*, Biomarker and pharmacologic evaluation of the gamma-secretase inhibitor PF-03084014 in breast cancer models. *Clin. Cancer Res.* **18**, 5008–5019 (2012).
50. X. H. Zhang *et al.*, Latent bone metastasis in breast cancer tied to Src-dependent survival signals. NCBI Gene Expression Omnibus. https://www.ncbi.nlm.nih.gov/geo/query/acc.cgi?acc=GSE14020. Deposited 17 December 2008.
51. T. Foukakis *et al.*, Gene expression profiling of sequential metastatic biopsies for biomarker discovery in breast cancer. NCBI Gene Expression Omnibus. https://www.ncbi.nlm.nih.gov/geo/query/acc.cgi?acc=GSE54323. Deposited 23 January 2014.
52. I. Espinoza, L. Miele, Notch inhibitors for cancer treatment. *Pharmacol. Ther.* **139**, 95–110 (2013).
53. S. A. Kahn *et al.*, Notch1 regulates the initiation of metastasis and self-renewal of group 3 medulloblastoma. *Nat. Commun.* **9**, 4121 (2018).
54. T. Xu *et al.*, RBPJ/CBF1 interacts with L3MBTL3/MBT1 to promote repression of Notch signaling via histone demethylase KDM1A/LSD1. *EMBO J.* **36**, 3232–3249 (2017).
55. R. Lehal *et al.*, Pharmacological disruption of the Notch transcription factor complex. *Proc. Natl. Acad. Sci. U.S.A.* **117**, 16292–16301 (2020).
56. V. Bolos *et al.*, Notch activation stimulates migration of breast cancer cells and promotes tumor growth. *Breast Cancer Res.* **15**, R54 (2013).
57. K. Wang *et al.*, PEST domain mutations in Notch receptors comprise an oncogenic driver segment in triple-negative breast cancer sensitive to a gamma-secretase inhibitor. *Clin. Cancer Res.* **21**, 1487–1496 (2015).
58. J. J. Quinn, H. Y. Chang, Unique features of long non-coding RNA biogenesis and function. *Nat. Rev. Genet.* **17**, 47–62 (2016).
59. S. Grelet *et al.*, A regulated PNUTS mRNA to lncRNA splice switch mediates EMT and tumour progression. *Nat. Cell Biol.* **19**, 1105–1115 (2017).
60. E. Grinman, Y. Nakahata, Activity-regulated synaptic targeting of lncRNA ADEPTR mediates structural plasticity by localizing Sptn1 and AnkB in dendrites. *Sci. Adv.* **7**, eabf0605 (2021).
61. L. Statello, C.-J. Guo, L.-L. Chen, M. Huarte, Gene regulation by long non-coding RNAs and its biological functions. *Nat. Rev. Mol. Cell Biol.* **22**, 96–118 (2020).
62. K. C. Wang, H. Y. Chang, Molecular mechanisms of long noncoding RNAs. *Mol. Cell* **43**, 904–914 (2011).
63. A. A. Sigova *et al.*, Transcription factor trapping by RNA in gene regulatory elements. *Science* **350**, 978–981 (2015).
64. S. Maddika *et al.*, WWP2 is an E3 ubiquitin ligase for PTEN. *Nat. Cell Biol.* **13**, 728–733 (2011).
65. W. H. Liu, H. W. Hsiao, W. I. Tsou, M. Z. Lai, Notch inhibits apoptosis by direct interference with XIAP ubiquitination and degradation. *EMBO J.* **26**, 1660–1669 (2007).
66. Z. Chen *et al.*, A tunable brake for HECT ubiquitin ligases. *Mol. Cell* **66**, 345–357.e6 (2017).
67. Q. Hu *et al.*, Oncogenic lncRNA downregulates cancer cell antigen presentation and intrinsic tumor suppression. *Nat. Immunol.* **20**, 835–851 (2019).